Convective and Oscillatory Losses in Q-Machines

by

Francis F. Chen

MATT-717 October 1969

PLASMA PHYSICS LABORATORY

Contract AT(30-1)—1238 with the
US Atomic Energy Commission

PRINCETON UNIVERSITY
PRINCETON, NEW JERSEY

Princeton University
Plasma Physics Laboratory
Princeton, New Jersey

Convective and Oscillatory Losses in Q-Machines

by

Francis F. Chen

MATT-717 October 1969

Paper presented at the International Conference on Physics of Quiescent Plasmas, Paris, September 8-13, 1969.

AEC RESEARCH AND DEVELOPMENT REPORT

This work was supported under Contract AT(30-1)-1238 with the Atomic Energy Commission.

CONVECTIVE AND OSCILLATORY LOSSES IN Q-MACHINES

Francis F. Chen[†]

Princeton University, Princeton, New Jersey

I. CONVECTIVE LOSSES

Previous measurements of the dependence of peak density n_p on input ion flux Φ_i in alkali-metal plasmas, summarized in /1/, have indicated an anomalous loss at low densities, even in uniform magnetic fields $\underline{B}$. This mysterious loss apparently arises from two causes: dc convection and low frequency oscillations. To separate these effects, we have added magnetic shear to stabilize the oscillations /1/. The results are summarized in Fig. 1, taken from Ref. 1, which shows n_p vs. the current I_s in the hard core providing the shear. All the experimental points lie below n_{cl}, the density expected if classical diffusion and endplate combination were the only loss processes. The curve n_{osc} is a lower limit to the density expected if the observed oscillation amplitude alone were responsible for the losses. At high shear, the oscillations are stabilized, and n_{osc} lies well above n_p, indicating the presence of a dc loss process. We have shown /1/ that this process is convection in asymmetric electric fields caused by temperature gradients in the endplates. Shear reduces this loss by twisting the equipotentials into long spirals, thus symmetrizing the $\underline{E} \times \underline{B}$ drifts. Fig. 2 shows the measured equipotentials at zero shear and with a small amount of shear. The observed twisting agrees well with a theory which assumes that potential is constant on a line of force. A detailed calculation of the convective loss rate /1/

[†]Present address: School of Engineering and Applied Science, University of California, Los Angeles, California 90024

produced the theoretical curve on Fig. 1; there is good agreement with experiment at high shear.

At low shear, the occurrence of oscillations causes n_p to lie below the theoretical curve. It is seen that at zero shear only about half of the losses can be attributed to convection; the other half is presumably connected with the oscillations.

II. OSCILLATORY LOSSES

1. Experimental method. We have attempted to relate the oscillation-induced losses to the detailed structure of the fluctuations. The experiment was carried out in a conventional Q-machine with no hard core and with central collimation of the neutral K beams. The plasma was 5 cm in diam and 326 cm long; B was around 2 kG. The fluctuation level was controlled by the previously reported /2, 3/ method of varying the aperture-limiter potential V_b.

Fig. 3 shows a graph of n_p and n_1/n_o vs. V_b, where n_1 is half the peak-to-peak density fluctuation measured where it is largest. There is a quiescent (Q) region where n_p is largest, a region of coherent oscillations, where n_p is slightly lower, and a region of turbulent fluctuations, where n_p suddenly drops by a factor of 3. Normally, with $V_b = 0$, we observe turbulent fluctuations; to recover the coherent drift waves reported by Hendel et al. /4/, we must set $v_b = 1.2V$. The position of the Q region of Fig. 3 depends on the contact potential of the limiter and on the uniformity of the endplate temperatures and apparently varies among Q-machines.

2. Subtraction of convective losses. The close relation between oscillation amplitude and loss rate apparent from Fig. 3 can be made more quantitative as follows. Particle balance requires

$$\Phi_i = \Phi_w + (A_c + A_f)\, n_p, \qquad (1)$$

where Φ_w is the endplate recombination loss /5/ computed from the measured density, and where we have assumed that convective and fluctuational losses

are proportional to n_p. Thus $A_c \approx 2\pi RLv_{convection}$ and $A_f \approx 2\pi RLD_\perp/\Lambda$, Λ being the density scale length. The value of A_c is found from the Q region, where $A_f = 0$. With the basic assumption that A_c remains constant, we can compute A_f for other values of V_b and plot it against $(n_1/n_o)_{max}$, as shown in Fig. 4. For turbulent fluctuations, A_f seems to vary as $(n_1/n_o)^3$; for coherent oscillations, A_f fits a $(n_1/n_o)^2$ law better. Note that points for the two turbulent regimes have been plotted separately, since A_c and Λ may actually vary with V_b.

3. Loss mechanisms. It is clear from Fig. 4 that there is an escape flux $\Phi_{osc} \equiv A_f n_p$ connected with the oscillation amplitude. The transport mechanism for coherent waves and for turbulent fluctuations may be quite different. For resistive drift waves of steady amplitude, the transport depends on the mechanism determining the nonlinear saturation and has been discussed by various authors /6-9/. For turbulent fluctuations, the transport can be computed from the statistical properties of the turbulence /10-12/, but it is nearly impossible to predict these properties. We find that there is an additional consideration which has not been recognized in previous studies of anomalous transport /13, 14/. This is that the oscillation amplitude, particularly of coherent waves, tends to be peaked inside the plasma and to become nearly zero at the boundary. Transport across the boundary can therefore occur only through secondary processes: 1) convection, 2) edge oscillations, or 3) scrape-off. In (1), the convective loss of Section I is enhanced because wave-particle scattering can transfer particles from closed equipotentials to those crossing the boundary. Furthermore, a large oscillation can modify the dc electric fields and change the value of A_c. In (2), the existence of a higher frequency Kelvin-Helmholtz instability /15/ near the edge can carry particles across the boundary if the amplitude envelopes of the two instabilities overlap. In (2), the finite radial excursion of particles oscillating in the wave can bring them outside the aperture. If their thermal motion now brings them closer to the endplate, where the amplitude is smaller, they cannot

swing back in the next half cycle and will eventually hit the limiter. Scrape-off cannot, however, occur in the absence of (1) and (2) if $E_r = 0$ at the edge.

4. Phase shift measurements. If A_c remains constant, the quantity $j_r = \langle \tilde{n}\, \tilde{v}_r \rangle$ gives the radial flux density due to oscillations regardless of the exact mechanism responsible for it. When $\tilde{v}_r = \tilde{E}_\theta/B$, the ion flux is directly measurable as

$$j_r = -\, i(m/r) \langle \tilde{n}\, \tilde{\phi} \rangle /B = \frac{1}{2}\,(m/rB)\,|n_1|\,|\phi_1|\,\sin\delta_o, \tag{2}$$

where $\underset{\sim}{E} = -\nabla\phi$ and δ_o is the phase angle by which $\tilde{n}$ leads $\tilde{\phi}$ in the $E_o = 0$ frame. Eq. (2) holds even for large oscillations because corrections to $\tilde{v}_r = \tilde{E}_\theta/B$ are of order $(\omega/\omega_{ci})^2 \ll 1$ /12/. A convenient formula for δ can be found from the electron continuity equation, which yields

$$\frac{e\phi_1}{KT} = \frac{n_1}{n_o}\,\frac{\omega - \omega_E + i\omega_{||}}{\omega^* + i\omega_{||}} \tag{3}$$

$$\operatorname{sgn}\omega \cdot \tan\delta = \frac{\omega_{||}\,[\omega^* - (\omega - \omega_E)]}{\omega_{||}^2 + \omega^*(\omega - \omega_E)}\,, \tag{4}$$

where $\omega^* = -(m/r)(KT/eB)(n_o'/n_o)$, $\omega_E = -(m/r)(E_r/B)$, and $\omega_{||} = k_{||}^2 (KT/eB)(B/n_o e\eta)$. Ion viscosity, finite r_L, and radial boundary conditions determine ω in a complicated way; but if the measured value of ω is used, Eq. (4) gives the local phase shift exactly. The factor sign ω takes into account the fact that, when ω_E is large and negative, δ will be negative ($\tilde{\phi}$ leads $\tilde{n}$) in the lab frame even though δ_o is positive and the flux is outward. Eqs. (3) and (4) show that $|n_1/\phi_1|$ and δ vary with r (we have observed this), so that the interpretation of phase shift measurements when $\omega_E \neq 0$ is not trivial.

5. Sinusoidal oscillations. Near threshold, as at $V_b = 1.9$V on Fig. 3, we observe /2, 3/ pure drift waves localized well inside the plasma. Our measurements of δ, which we cannot show here, are smaller than those reported by Hendel et al. /4/ and similar to those of Rowberg and Wong /16/. Perhaps the difference can be attributed to our small value of $\omega_{||}/\omega^* \approx 0.2$

[see Eq. (4)] and to the use of the method of driven shields /17/ to measure $\tilde{\phi}$. Our interpretation of the meaning of j_r differs somewhat from that of Hendel et al. /4/. Since $n_1 \approx 0$ at the boundary, the radial losses due to the wave are extremely small, as Fig. 10a of Ref. 4 clearly shows. Measurements of δ and j_r in the interior, however, show an outward flux which has the effect of decreasing the center density and increasing slightly the density at large radii. This flux is taken up by an adjustment of the endplate recombination distribution. Thus what was observed in /4/ was primarily not a radial loss but merely a redistribution of the end losses. What little flux did cross the boundary was due to the secondary effects enumerated in Section II3.

This is not to say, however, that the drift instability cannot cause radial losses. The wave is sinusoidal precisely because the end losses can take up the interior radial flux and because a reflecting radial boundary condition creates a radial standing wave. If either condition were removed, such as in a torus, the radial flux would appear at the boundary; but then the wave would no longer be a pure mode.

6. Large periodic oscillations. In addition to sinusoidal waves with a "soft" onset, we sometimes observe large oscillations with a "hard" onset /7/. An example is shown in Fig. 5, which shows $n_p(r=0)$ and $\tilde{E}_\theta$ (r=1.2 cm), taken with a double floating probe, as a function of V_b. As V_b is increased from the Q region, a small 6 kHz oscillation develops at $V_b \approx 3.5$ V; this has practically no effect on n_p. At $V_b \approx 7.5$ V, n_p drops as turbulent oscillations with a strong 1 kHz component appear. If V_b is now reduced, the continuous spectrum changes to a line spectrum, corresponding to a large periodic oscillation with a 1.3 kHz fundamental. This disappears abruptly when V_b is reduced below 3V. The waveforms and density profiles are shown in Fig. 6. The 6 kHz oscillation is an m=3 drift wave near threshold, its amplitude being determined by the quasilinear terms in the amplitude equation. The 1.3 kHz oscillation, on the other hand, appears to be a truly nonlinear

solution, of the type discussed by Hooper /18/, which cannot be found by corrections to the linear solutions. It distorts the density profile and apparently causes large anomalous transport. The "hysteresis" in Fig. 5 is typical of nonlinear systems with a bifurcation point.

We have measured δ for both oscillations at $V_b \approx 3.6$ V and r=1.2 cm. The 6 kHz oscillation has $\delta = 6\pm3^o$ and $n_1/n_o = .08$; this yields a value of j_r in agreement with the small change in n_p shown in Fig. 6. It is likely, however, that the change in convective loss is of comparable magnitude. The measurement of δ for the 1.3 kHz m=1 oscillation is shown in Fig. 7, which is a Lissajous figure with $\tilde{n}$ displayed vertically and $\tilde{\phi}$ horizontally. From the width of the trace, one obtains $\delta = 15^o.5$ for the fundamental and $\delta = 7^o.6$ for the harmonic. With $n_1/n_o \approx 0.35$, Eq. (2) then predicts $e\Phi_{osc} \approx 1.4$ mA. If Eq. (1) is used to subtract out the convective losses, the change in n_p yields $e\Phi_{osc} \approx 6.6$ mA. In this case, the $<\tilde{n}\,\tilde{v}_r>$ flux does not account for the enhanced losses; the oscillation apparently causes increased convective losses by changing the plasma symmetry.

The radial variation of δ was measured on another run with a hard-onset oscillation. The radial profiles of floating potential V_f, density, and n_1/n_o are shown in Fig. 8, and the waveform in Fig. 9. Note that n_1/n_o is peaked nearer the boundary than is the case for small sinusoidal oscillations. From Fig. 8, one can compute $\omega^*(r)$, $\omega_{||}(r)$, $\omega_E(r)$ and, therefore, $\delta(r)$ from Eq. (4). The measured values of ω and $k_\perp$ were used. The curve in Fig. 9 shows the calculated phase shifts; the points are the directly measured phase shifts. There is agreement to the extent that, since ω_E is large and negative and $\omega < 0$, we have $\delta \leqq 0$ everywhere except near the axis, where ω_E became small. However, the large predicted phase shifts of 50^o-70^o could not be observed. If one takes $\delta = -70^o$, Eq. (2) yields $e\Phi_{osc} \approx 3.4$ m A at the oscillation peak. The value computed from Δn_p and Eq. (1) is $e\Phi_{osc} = 4.5$ m A. If one takes the maximum measured shift $\delta = -20^o$, however, one obtains $e\Phi_{osc} \leqq 1.2$ m A; and one again concludes that the $<\tilde{n}\,\tilde{v}_r>$ flux

is insufficient to account for the enhanced losses.

7. Turbulent fluctuations. For the various turbulent regimes at $V_b = 0, -2, \pm 4$, and ± 8-10V, we measured the profiles $n(r)$, $\langle \tilde{n}^2(r) \rangle$, and $\langle \tilde{\phi}^2(r) \rangle$; the frequency spectra $S(\omega, r)$; the density autocorrelation function $C(\tau)$ and the propagation velocity from $C(\tau, \Delta\theta)$; the $\tilde{n} - \tilde{\phi}$ cross-correlation; the $\tilde{n} - \tilde{\phi}$ phase shift δ; and the quantity $\langle \tilde{n} \tilde{E}_\theta \rangle$. The last was measured with three probes and the PAR Model 100 Correlator. Fluctuation intensities were measured with a biased-diode true mean-square meter. The principal results are as follows:

a) The amplitude envelopes of turbulent fluctuations extend to the boundary, so that transport across the boundary is easily accomplished by the oscillations. Fig. 10 shows radial profiles of $n_o(r)$ and $\tilde{n}_{rms}/n_o$ in the frequency range 5 Hz-500 kHz for $V_b = -2$ and +4 V. In both cases the low-frequency envelope overlaps that of the "edge oscillation."

b) The degree of randomness increases with $|V_b|$. Fig. 11 shows the frequency spectrum, autocorrelation function, and $\tilde{n}$ traces from two probes 90^o apart for $V_b = 0$ and -2 V. With increasing distance from threshold the spectrum extends to higher frequencies, the periodic oscillation in $C(\tau)$ is lost, and the correlation length is shortened so that the two probe traces are no longer identical except for a shift. The spectrum does not vary greatly with radius.

c) Abrupt decreases in density are accompanied by a spreading of the spectrum to very low frequencies. This is illustrated by Fig. 12, which shows the $\tilde{n}$ spectrum at $r \approx 0.9$ cm and $V_b = +4$, 7.7, and 10 V (see Fig. 5). At $V_b = 4$ V, where the density is high, there is only the coherent 6 kHz oscillation shown in Fig. 6; there are no fluctuations below 1 kHz (the zero peak is instrumental). At $V_b = 7.7$ V, the density has dropped by a factor of 3 (Fig. 5), and the spectrum shows a spreading to $f < 1$ kHz. Going to $V_b = 10$ V, one finds that the density and oscillation amplitude are not greatly changed (Fig. 5), although the spectrum above 1 kHz appears entirely

different. It appears that the large anomalous loss is controlled mainly by the frequencies below the drift frequency.

d) $\tilde{n}-\tilde{\phi}$ phase shifts for large turbulent fluctuations are rather small. Direct oscilloscope traces of $\tilde{n}$ and $\tilde{\phi}$ (Fig. 13) show no discernible delay, but δ can be measured roughly from Lissajous figures. In Fig. 14 we show the $\tilde{n}-\tilde{n}$ and $\tilde{n}-\tilde{\phi}$ Lissajous figures for $V_b = 0$, -10, and +10V. At $V_b = 0$, the increased broadening of the ellipse yields $|\delta| \approx 15^o$. At $V_b = -10$ V, the oscillations are so large the $\tilde{n}-\tilde{\phi}$ Lissajous figure is curved because of the exponential dependence of n on ϕ. The broadening shows $|\delta| \approx 1^o.5$. At $V_b = +10$ V, the oscillations have a different character, $|\delta|$ being larger for positive excursions ($|\delta| \approx 11^o$) than for negative ($\delta \approx 0$). One can compute Φ_{osc} from these values of $|\delta|$ and the measured amplitudes and correlation lengths. The resulting values of Φ_{osc} are in general two small to account for the decrease in density, but this method of measuring Φ_{osc} is rather inaccurate.

e) The nature of the turbulence is different for the $V_b < 0$ and $V_b > 0$ regimes. This is apparent from the $\tilde{n}-\tilde{\phi}$ Lissajous figures (Fig. 14), the radial amplitude distribution (Fig. 10), and the density profiles (Fig. 15). A large anomalous loss is observed in both regimes, but the details of the transport mechanism appear to be different.

f) Oscillatory transport accounts for the density decrease in the turbulent regime. To measure that accurately, we took the cross-correlation between $\tilde{n}$ and $\tilde{E}_\theta$, using two floating probes ($\Delta\theta = 10^o$) and a differential amplifier to obtain $\tilde{E}_\theta$. Fig. 16 shows $C(\tau)$ taken with the PAR Model 100 Correlator when $\tilde{n}-\tilde{n}$, $\tilde{E}_\theta-\tilde{E}_\theta$, $\tilde{n}-\tilde{E}_\theta$, and $\tilde{E}_\theta-\tilde{n}$ were successively applied to the two input channels. The probes were located at $r \approx 2$ cm (near the edge), and the conditions were: $B = 2160$ G, $e\Phi_i = 10$ m A, $n_p = 7.0 \pm 0.3 \times 10^{10}$ cm^{-3}, $e\Phi_w = 0.5$ m A, $e\Phi_{convection} = 1.9$ m A. The $\langle \tilde{n}\tilde{n} \rangle$ and $\langle \tilde{n}\tilde{E}_\theta \rangle$ signals were calibrated absolutely. Frequency response was approximately 5 Hz - 200kHz. If j_r is assumed uniform over the plasma surface, the observed value of

$\langle \tilde{n}\tilde{E}_\theta \rangle$ (Fig. 16) yields $e\Phi_{osc} = 7.5$ m A, compared to $\Phi_{osc} = \Phi_i - \Phi_w - \Phi_{conv} = 7.6/e$ m A. A change in A_c need not be postulated to explain the observed losses.

III. CONCLUSION

Anomalous transport in Q-machines is caused partially by DC convection and partially by oscillations. Pure drift waves can account for only a small radial loss because their amplitude is small at the boundary. Large nonlinear oscillations can cause a large loss by increasing the dc convection. Turbulent fluctuations can carry plasma across the boundary easily and also cause a large loss when the spectrum extends to low frequencies (not necessarily dc). We made an effort to confirm these conclusions by direct measurements of the radial flux by means of a plasma-eater, but the data did not give self-consistent results.

We have benefited from enlightening discussions with Drs. K. Bol, T.K. Chu, W. Horton, F. Perkins, and H. Wobig. Professor K.C. Rogers and Dr. D. Mosher participated in experiments which led to the present measurements. This work was supported by the U.S. Atomic Energy Commission under Contract AT(30-1)-1238.

REFERENCES

/1/ D. Mosher and F. F. Chen, Princeton MATT-691 (1969), submitted to Phys. Fluids.

/2/ F. F. Chen, D. Mosher, and K. C. Rogers, Plasma Physics and Controlled Nuclear Fusion Research (Novosibirsk Conference, 1968), Vol. I, p. 625 (International Atomic Energy Agency, Vienna, 1969).

/3/ K. C. Rogers and F. F. Chen, Princeton MATT-695 (1969), submitted to Phys. Fluids.

/4/ H. W. Hendel, T. K. Chu, and P. A. Politzer, Phys. Fluids 11, 2426 (1968).

/5/ R. W. Motley and D. L. Jassby, Phys. Rev. Letters 22, 333 (1969).

/6/ F. F. Chen, Phys. Fluids 8, 912 (1965).

/7/ B. B. Kadomtsev, Plasma Turbulence (Academic Press, New York, 1965).

/8/ T. H. Dupree, Phys. Fluids 11, 2680 (1968).

/9/ T. H. Stix, Phys. Fluids 12, 627 (1969).

/10/ L. Spitzer, Jr., Phys. Fluids 3, 659 (1960).

/11/ T. H. Dupree, Phys. Fluids 10, 1049 (1967).

/12/ T. H. Stix, Phys. Fluids 10, 1601 (1967).

/13/ K. I. Thomassen, Phys. Fluids 9, 1836 (1966).

/14/ M. Porkolab and G. S. Kino, Phys. Fluids 11, 346 (1968).

/15/ G. Kent, N. Jen, and F. F. Chen, Phys. Fluids (to be published).

/16/ R. E. Rowberg and A. Y. Wong, Phys. Fluids (to be published).

/17/ F. F. Chen, Proceedings of Conference on Physics of Quiescent Plasmas, Frascati, 1967, Vol. II, p. 563.

/18/ E. B. Hooper, Phys. Fluids (to be published).

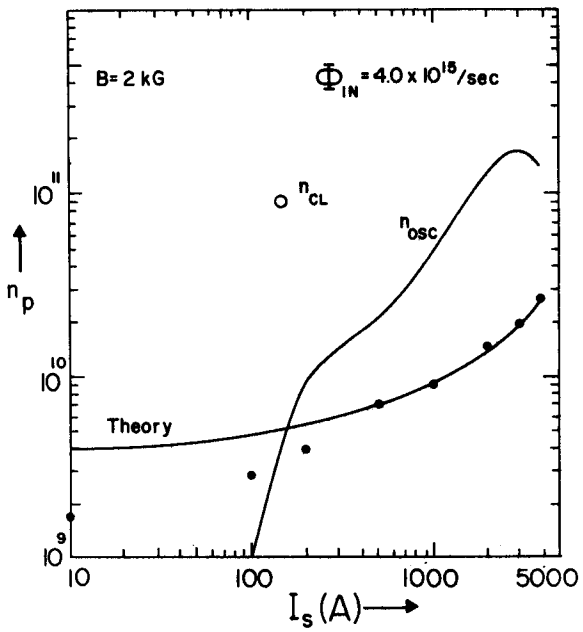

Figure 1

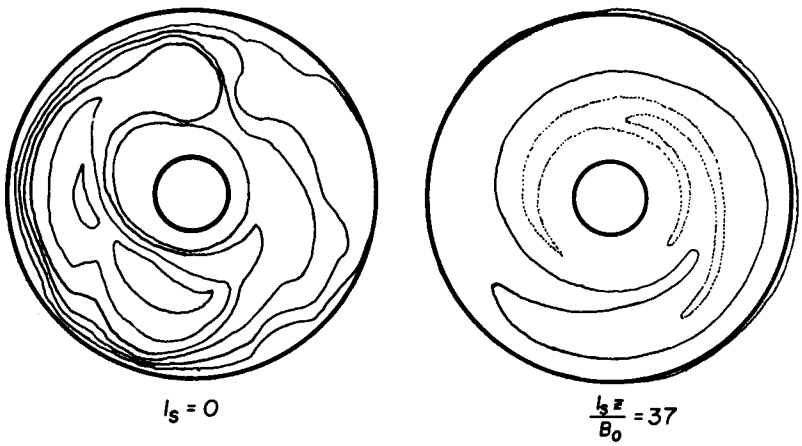

Figure 2

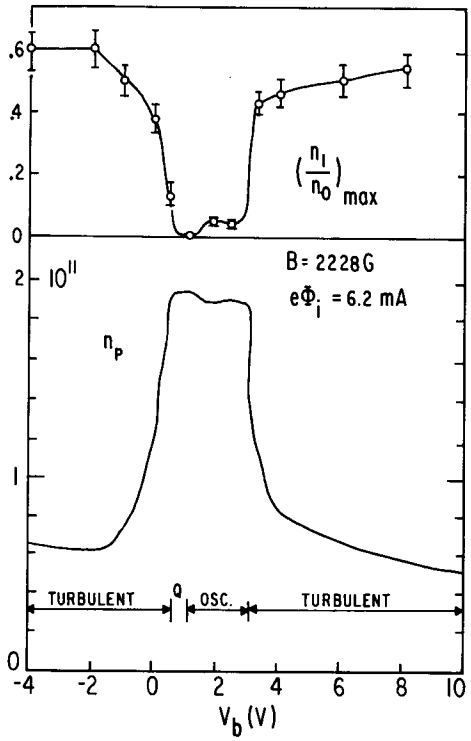

Figure 3

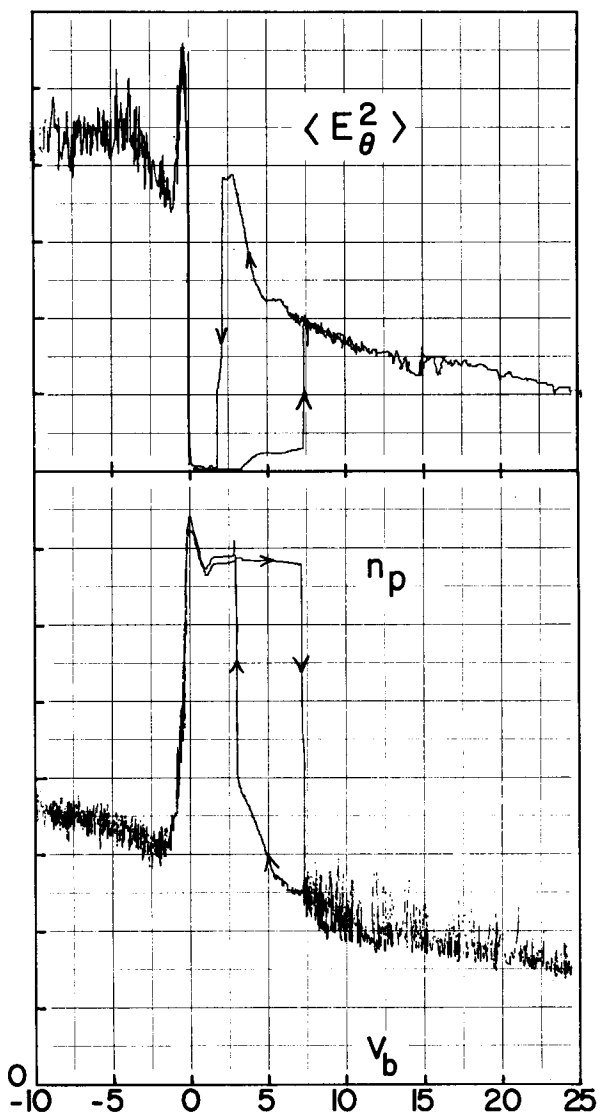

Figure 5

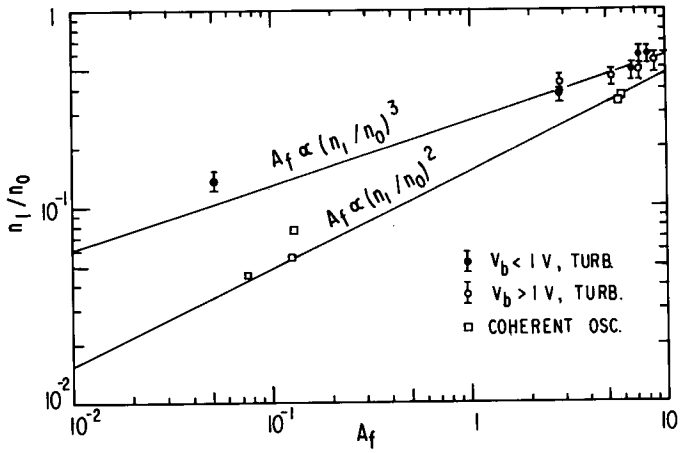

Figure 4

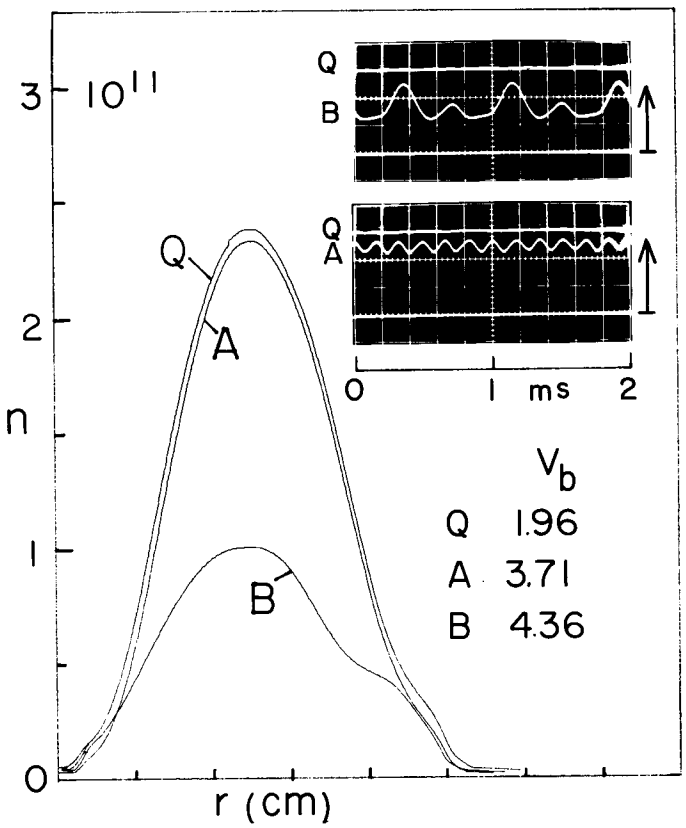

Figure 6

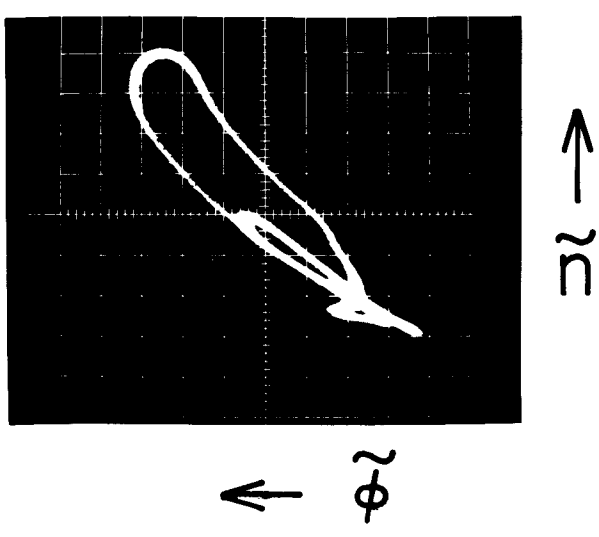

Figure 7

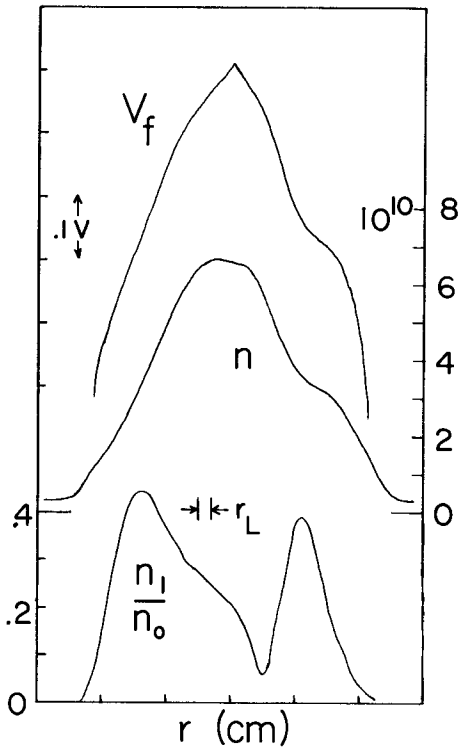

Figure 8

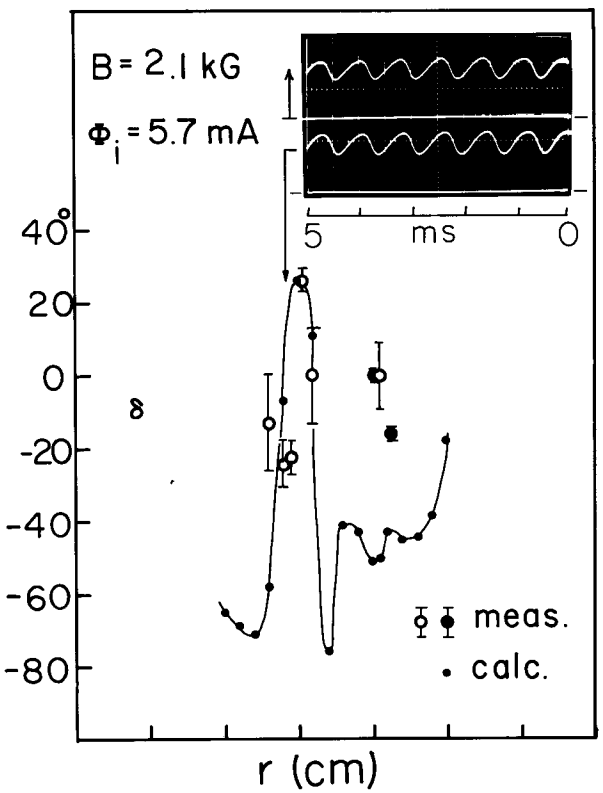

Figure 9

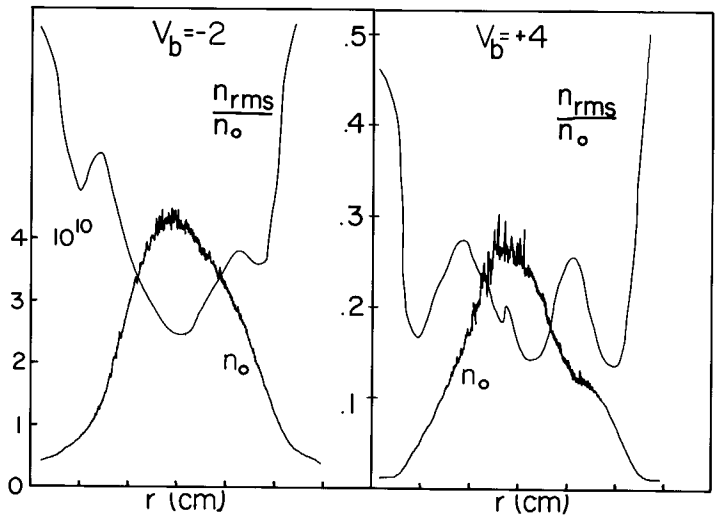

Figure 10

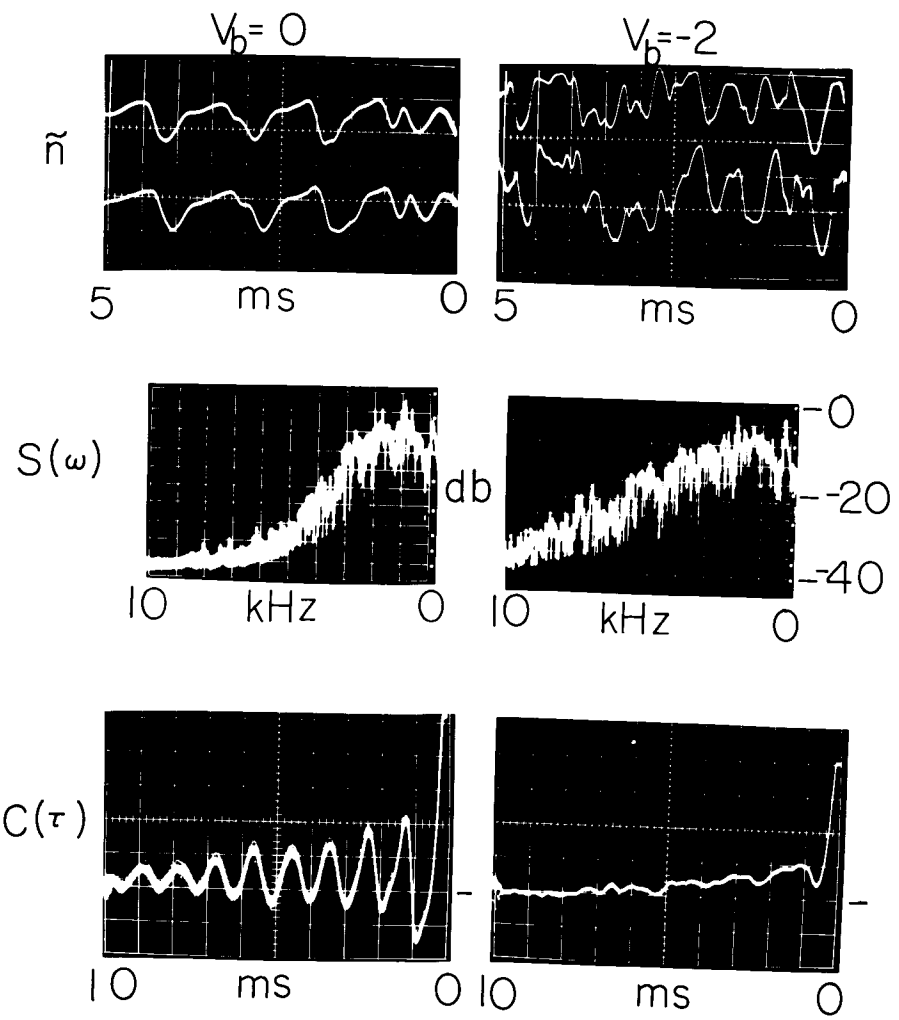

Figure 11

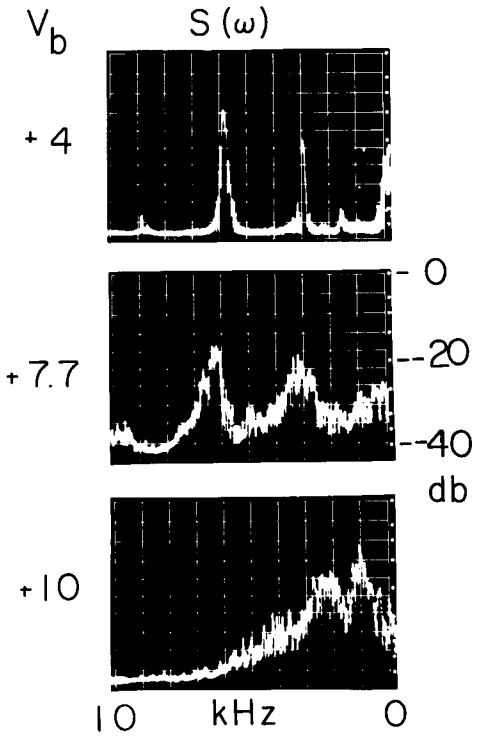

Figure 12

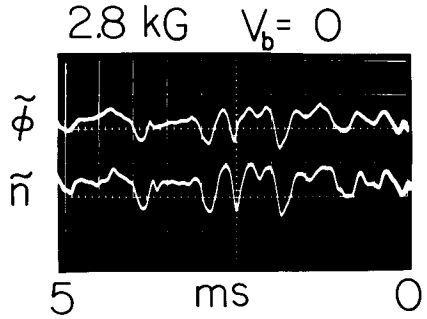

Figure 13

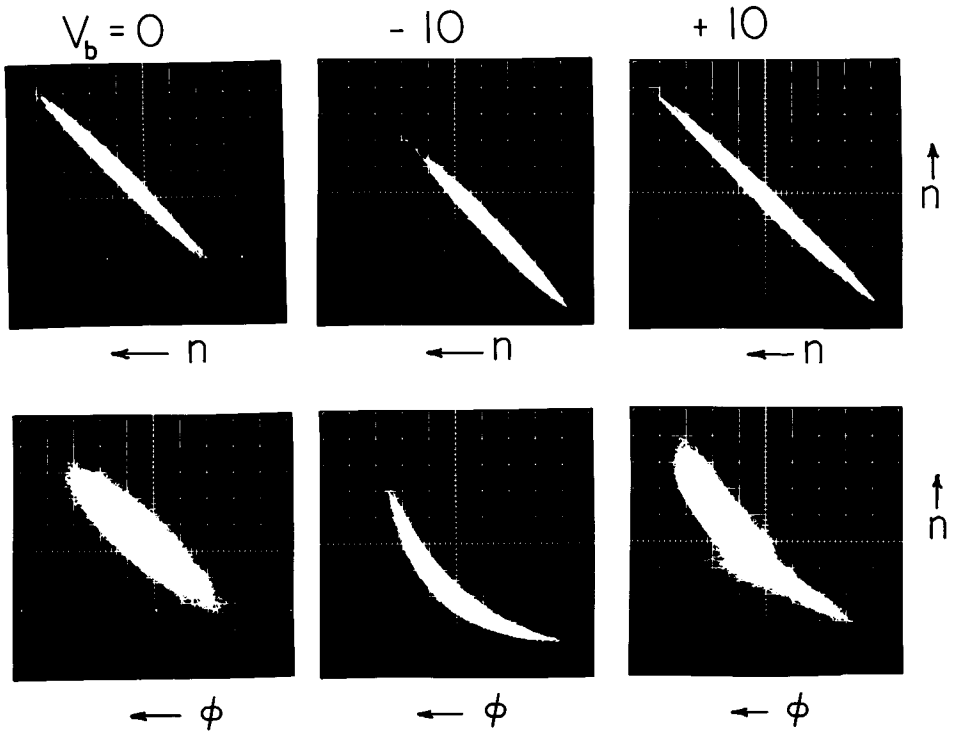

Figure 14

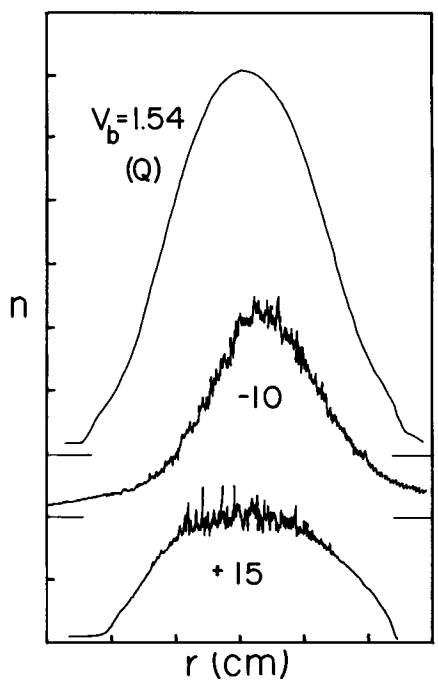

Figure 15

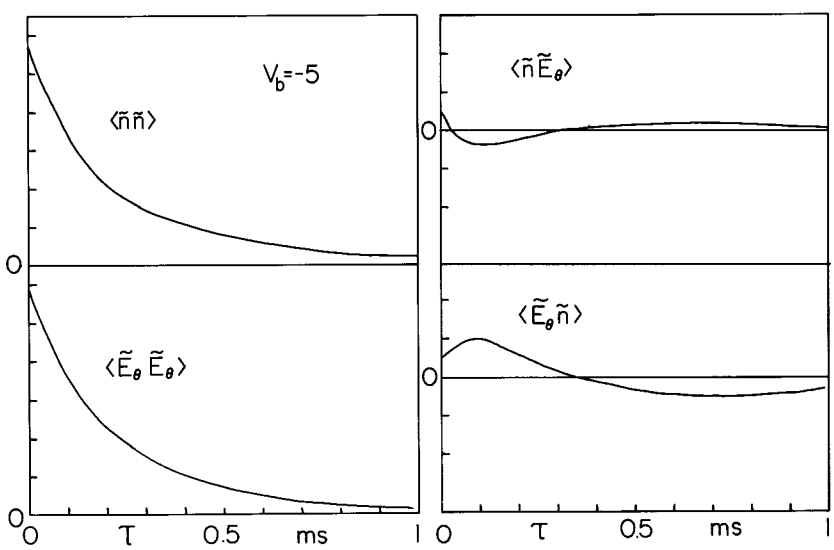

Figure 16